ACS OMEGA

Open Access

http://pubs.acs.org/journal/acsodf

Article

Synthesis of the Novel *N*-(2-Hexadecynoyl)-L-Homoserine Lactone and Evaluation of Its Antiquorum Sensing Activity in *Chromobacterium violaceum*

David J. Sanabria-Ríos,* Rene García-Del-Valle, Sachel Bosh-Fonseca, Joangely González-Pagán, Alanis Díaz-Rosa, Karina Acevedo-Rosario, Luzmarie Reyes-Vicente, Antonio Colom, and Néstor M. Carballeira

Cite This: *ACS Omega* 2024, 9, 32536−32546

Read Online

ACCESS | Metrics & More | Article Recommendations | Supporting Information

ABSTRACT: *Chromobacterium violaceum* is commonly found in soil and freshwater within tropical and subtropical regions. Although not a common occurrence, this bacterium has the potential to cause severe diseases in humans and animals, such as liver and lung abscesses and septicemia. Herein we report the synthesis of novel *N*-acyl homoserine lactones (HSLs) to evaluate their effectiveness as antiquorum sensing (anti-QS) agents in *C. violaceum*. The HSLs were prepared through three synthetic approaches, where hexanoic acid, decanoic acid, 6-decynoic acid, or 2-hexadecynoic acid (2-HDA) was treated with commercially available L-homoserine lactone (HSL) hydrobromide in either dichloromethane or tetrahydrofuran in the presence of EDC and DMAP. The effectiveness of HSLs as anti-QS agents was assessed through susceptibility tests and violacein quantification. The most effective anti-QS inhibitor among all *N*-acyl-HSLs tested was the *N*-(2-hexadecynoyl)-L-homoserine lactone (HSL **4**). Further experimental approaches, such as quantification of acyl-homoserine lactones and biofilm inhibitory tests, were carried out to determine the effect of HSL **4** on these QS-dependent mechanisms. These experiments showed that HSL **4** was highly effective at inhibiting the production of HSLs and biofilm in *C. violaceum* at 0.25, 0.50, and 1 mg/mL. In addition, the cytotoxicity activity was evaluated against Vero cells to determine the selectivity of HSL **4** as a nontraditional antibacterial agent. HSL **4** was not toxic against Vero cells at concentrations ranging from 0.0039 to 1 mg/mL. Molecular docking experiments were conducted to study the interactions between novel HSLs and CviR (PDB ID 3QP5), a receptor that plays a significant role in *C. violaceum* QS. *In silico* studies indicate that HSL **4** exhibits better interactions with Leu 72 and Gln 95 of the CviR binding pocket when compared to the other analogs. These results validate previous *in vitro* studies, such as susceptibility tests and violacein production assays. The findings above indicate that novel acetylenic HSLs may potentially be agents that combat bacterial communication and biofilm formation. However, further investigation is necessary to expand the spectrum of bacterial strains capable of resisting antibiotics through QS and evaluate the compounds' cytotoxicity in other cell lines.

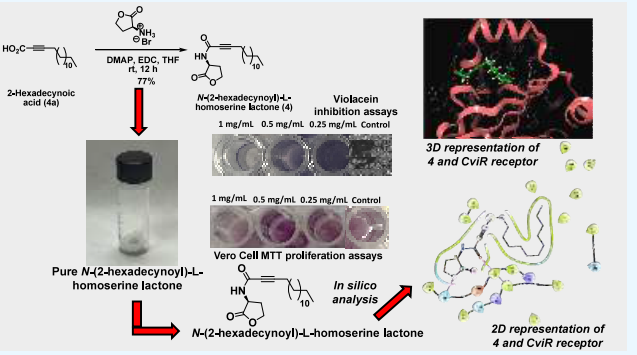

INTRODUCTION

Chromobacterium violaceum is a soil and freshwater Gram-negative bacillus found in tropical and subtropical regions.[1,2] On rare occasions, this microorganism can be an opportunistic pathogen in animals and humans, causing liver and lung abscesses and fatal septicemia due to an initial skin lesion.[1,3] One peculiarity of *C. violaceum* is its ability to produce violacein, a violet nondiffusible antimicrobial pigment.[4] Violacein production involves the expression of the vio operon consisting of five enzyme coding genes, namely, *vioA*, *vioB*, *vioC*, *vioD*, and *vioE*, transcribed in one direction.[5,6] A 7.3 kb long DNA fragment codes these enzymes.[5]

Extensive reports have demonstrated that the generation of violacein in *C. violaceum* is a process that depends on quorum sensing (QS).[7−12] QS in bacteria regulates gene expression as a response to variations in cell-population density through the production and release of chemical signals known as autoinducers.[13] The higher the population of bacteria, the higher the concentration of autoinducers.[13] Through QS, bacteria can regulate the expression of several collective functions, including the production of multiple virulence

Received: February 4, 2024
Revised: July 4, 2024
Accepted: July 11, 2024
Published: July 22, 2024

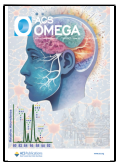

factors, antibiotic production, bioluminescence, biofilm formation, and swarming motility, once a population threshold is reached.[14,15]

C. violaceum has a QS system, the CviR receptor, that is regulated by the C6-homoserine lactone (C6-HSL) autoinducer **1** displayed in Figure 1.[7,16] Recently, a crystallographic

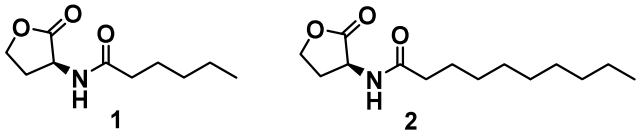

Figure 1. Chemical structures of C6-HSL (**1**) and C10-HSL (**2**).

study done with CviR and different HSLs confirmed that minor changes to the natural autoinducer (e.g., increase in the carbon chain length in the acyl moiety to 10C) can change the modulation activity of the HSL into an antagonist in the presence of C6-HSL.[17]

Inhibition of QS has emerged as a promising strategy to combat bacterial infections without exerting selective pressure to develop resistance.[18] *N*-Acyl HSLs are key signaling molecules involved in QS, making them attractive targets for developing anti-QS agents. Several compounds have been tested as inhibitors of QS in *C. violaceum*.[19−21] Some compounds include methyl eugenol, sappanol, butein, bavachin, catechin 7-xyloside, kitasamycin, and nitrofurantoin.[19−21] In 2001, Ikeda et al. reported the synthesis of optically pure enantiomers of *N*-acyl HSL autoinducers.[22] They determined that L-isomers displayed significant anti-QS activity, while no effect was observed with D-isomers.[22] On the other hand, Chhabra and colleagues performed the total synthesis of the bacterial *N*-(3-oxododecanoyl)-L-HSL[23] and McClean et al., in another study, reported that this compound, and other related *N*-acyl HSL analogs displayed anti-QS activity in *C. violaceum* (CV026), with C10-HSL being the most active inhibitor of QS (Figure 1).[7] In this context, synthesizing novel acyl HSLs presents an opportunity to explore their potential as QS activity inhibitors with QS-dependent mechanisms. There is a critical need to develop novel therapeutic agents to combat bacterial infections and overcome the challenges of antibiotic resistance. Thus, synthesizing and evaluating compounds with anti-QS properties can contribute significantly to filling this gap in the field.

In the present study, we aim to investigate the anti-QS properties of novel HSLs and their potential to suppress QS-regulated mechanisms such as biofilm formation and AHL generation in *C. violaceum*. The selection of novel *N*-alkynoyl-HSLs, particularly HSL **4**, is well-justified based on their unique structural modifications, including triple bonds at specific positions in the acyl moiety. Such changes have been shown to impact the anti-QS activity of these compounds, making them promising candidates for further evaluation. This study involves conducting various experiments such as susceptibility tests, quantification of violacein, quantification of *C. violaceum*'s AHLs, quantification of biofilm formation, and evaluation of the cytotoxicity activity of HSL **4** on Vero cells. Vero cells are commonly used in toxicity studies to evaluate the safety of potential therapeutic agents, as they have rapid growth and reproducibility in culture and are similar to human epithelial cells. Through a combination of *in vitro* and *silico* analyses, we assessed the efficacy of synthetic *N*-acyl-HSLs for reducing violacein production and inhibiting biofilm formation. Additionally, we explore the molecular interactions between the synthesized compounds and the CviR receptor, providing insights into their mechanism of action. The results from the experiments above will provide relevant information regarding the selectivity of these compounds and their potential as antibacterial agents. Such studies are critical in understanding the mechanisms of action of potential infections, ultimately helping develop new therapeutic agents to combat antibiotic resistance and bacterial pathogenicity.

MATERIALS AND METHODS

The glassware was sealed correctly with a rubber septum and flame-dried under a positive argon (Ar) or nitrogen (N_2) stream. The experimental setup consisted of a septum-sealed bottomed flask, a magnetic bar, and a stirrer. The tetrahydrofuran (THF), 1,3-dimethyl-2-imidazolidinone (DMI), dichloromethane (DCM), and *N*,*N*-dimethylformamide (DMF) were obtained from Sigma-Aldrich, dried, and protected with an Aldrich Sure/Seal System. FT-IR data were gathered on a Thermo Scientific Nicolet iS5 FT-IR spectrophotometer. All the products were characterized by ^{1}H NMR and ^{13}C NMR using a Nanalysis 100 Pro, Bruker Avance DPX-300, or Bruker Advance DRX-500 system. The NMR samples were prepared in $CDCl_3$, and the signals observed at 7.26 ppm (^{1}H NMR) and 77.16 ppm (^{13}C NMR) were used as internal standards. Minimal inhibitory concentration (MIC), violacein production, HSL formation, biofilm formation, and MTT cell proliferation OD values were spectrophotometrically measured using a Varioskan LUX multimode microplate reader (Thermo Scientific) at 600, 585, 520, and 570 nm, respectively. Vero Kidney African Green Monkey (CCL-81) was purchased from the American Type Culture Collection (Manassas, VA, USA).

Total Synthesis of Novel Acyl HSLs. *Synthesis of 6-Decynoic Acid (**3c**). 6-Decynol (**3b**).* Commercially available 1-heptynol (**3a**) was treated with 3,4-dihydro-2*H*-pyran (DHP) under *p*-toluenesulfonic acid (PTSA) catalytic conditions. Then, the resulting tetrahydropyranyl-protected alkynol was reacted with 1-bromopropane to obtain 2-(6-decynyl-1-oxy)-tetrahydro-2*H*-pyran. To a 50 mL round-bottomed flask were added 2-(6-decynyl-1-oxy) tetrahydro-2*H*-pyran (1.2 g, 5.0 mmol), catalytic amounts of PTSA, and 20 mL of methanol (MeOH). The stirring solution was refluxed at 65 °C for 12 h. After the reaction, the solvent was removed *in vacuo*; the crude reaction was washed with a $NaHCO_3$ saturated aqueous solution (2 × 10 mL), extracted with diethyl ether (2 × 15 mL), dried over $MgSO_4$, and filtered. The solvent of the filtered solution was removed *in vacuo*. The pale-yellow liquid was purified using silica gel column chromatography, eluting **3b** with hexane/ether (7:3). Alcohol **3b** (0.5 g, 3.1 mmol) was obtained as a colorless oil in a 73% yield. The spectroscopic data gathered for **3b** are in complete agreement with the spectroscopic data reported in the literature for this compound.[24−26]

*6-Decynoic Acid (**3c**).* To a 50 mL round-bottomed flask, under argon, were added 5.5 g (14.5 mmol) of pyridinium dichromate (PDC) and 20 mL of dry dimethylformamide (DMF). To the stirring solution was added 0.4 g (2.9 mmol) of **3b**, and the reaction mixture was left stirring for 48 h. After the reaction time, the crude was filtered using silica gel and diethyl ether as eluent. The solvent of the filtered solution was removed *in vacuo*. The obtained yellowish liquid was purified using silica gel column chromatography, eluting the 6-decynoic

https://doi.org/10.1021/acsomega.4c01121
ACS Omega 2024, 9, 32536−32546

acid (**3c**) with hexane/ether (7:3). Acid **3c** (0.3 g, 1.8 mmol) was obtained as a colorless oil for a 88% yield. FT-IR spectroscopic data for **3c** were identical to what was reported in the literature for this compound.[27] ^{1}H NMR (300 MHz, $CDCl_3$) δ (ppm) 2.41−2.36 (2H, t, J = 6.4 Hz, H-2), 2.22−2.08 (4H, m, H-5, H-6), 1.80−1.44 (6H, m, $-CH_2-$), 0.99-0.94 (3H, t, J = 7.0 Hz, $-CH_3$); ^{13}C NMR (75 MHz, $CDCl_3$) δ (ppm) 179.28 (s, C-1), 80.62 (s, C- 6), 79.42 (s, C-7), 33.43 (t, C-2), 28.37 (t), 23.79 (t), 22.45 (t), 20.71 (t), 18.40 (t), 13.42 (q, C-10).

Methyl 6-Decynoate. GC/MS (70 eV) m/z (relative intensity): 182 (M+, 0.01), 150 (16), 135 (8), 122 (26), 108 (46), 93 (50), 79 (100), 67 (43), 59 (19), 55 (19).

*Synthesis of 2-HDA (**4a**).* Compound **4a** was synthesized, purified, and characterized as described in the literature.[28,29]

Synthesis of N-Acyl-L-homoserine Lactones. A mixture of alkanoic or alkynoic FAs and L-homoserine lactone (HSL) hydrobromide (Sigma-Aldrich, Missouri, USA) was prepared in either dichloromethane (DCM, 15 mL) or tetrahydrofuran (THF, 15 mL) and stirred at room temperature for 15 min. Then, the dropwise addition of *N*-(3-(dimethylamino)propyl)-*N*′-ethylcarbodiimide (EDC, Sigma-Aldrich, Missouri, USA) was carried out. The reaction mixture was left stirring for 24 h and later washed with 5% (v/v) HCl aqueous solution (2 × 10 mL) and extracted with DCM or ethyl acetate (3 × 10 mL). The organic phase was dried over $MgSO_4$ and filtered, and the solvent was removed *in vacuo*. The crude was purified using silica gel column chromatography eluting with DCM/MeOH (19:1) or DCM/EtOAc (19:1).

N-(Hexanoyl)-L-homoserine Lactone (C6-HSL). C6-HSL was obtained as a white solid in 86% yield from the reaction of commercially available **1a** (0.50 g, 4.30 mmol), DMAP (0.2 g, 1.72 mmol), HSL (0.52 g, 2.87 mmol), and EDC (0.8 mL, 4.30 mmol) in DCM (15.0 mL) following the general procedure described above. FT-IR and NMR spectroscopic data are consistent with those reported in the literature.[30]

N-(Decanoyl)-L-homoserine Lactone (C10-HSL). C10-HSL was obtained as a white solid in 79% yield from the reaction of commercially available **2a** (0.28 g, 1.65 mmol), DMAP (0.08 g, 0.66 mmol), HSL (0.20 g, 1.10 mmol), and EDC (0.29 mL, 1.65 mmol) in DCM (10.0 mL) following the general procedure described above. Both FT-IR and NMR data of **2** were identical to what was reported in the literature.[23,30]

*N-(6-Decynoyl)-L-homoserine Lactone (HSL **3**).* HSL **3** was obtained as a white solid in 59% yield from the reaction of **3c** (0.10 g, 0.59 mmol), DMAP (0.04 g, 0.36 mmol), HSL (0.12 g, 0.65 mmol), and EDC (0.16 mL, 0.89 mmol) in DCM (10.0 mL) following the general procedure described above. Mp (°C) 110−112 °C; IR (neat) ν_{max} 3315 (−NH−), 2959, 2936, 2865, 2490, 1775, 1643, 1548, 1381, 1360, 1174, 1014 cm^{-1}; ^{1}H NMR (100 MHz, $CDCl_3$) δ (ppm) 6.06 (1H, s, −NH−), 4.67−4.14 (1H, m), 2.99−2.71 (2H, m), 2.20 (2H, m), 2.21−2.04 (4H, m), 1.90−1.25 (7H, m), 0.96 (3H, t, J = 7.2 Hz); ^{13}C NMR (26 MHz, $CDCl_3$) δ (ppm) 175.57 (s), 173.50 (s, C-1), 80.65 (s), 79.53 (s), 66.03 (t), 49.23 (d), 35.56 (t), 30.56 (t), 28.45 (t), 24.49 (t), 22.41 (t), 20.66 (t), 18.40 (t), 13.35 (q). HRSMS-APCI (m/z): $[M + H]^+$ calcd for $C_{14}H_{22}O_3N$ 252.1594, found 252.1593.

*N-(2-Hexadecynoyl)-L-homoserine Lactone (HSL **4**).* HSL **4** was obtained as a white solid in 77% yield from the reaction of 2-HDA (0.28 g, 1.11 mmol), DMAP (0.04 g, 0.30 mmol), HSL (0.14 g, 0.74 mmol), and EDC (0.20 mL, 1.11 mmol) in THF (10.00 mL) following the general procedure described above. Mp (°C) 93−95 °C; (neat) ν_{max} 3292 (−NH−), 2920, 2850, 2236, 1778, 1630, 1540, 1382, 1360, 1175, 1012 cm^{-1}; ^{1}H NMR (100 MHz, $CDCl_3$) δ (ppm) 6.3 (1H, s, −NH−), 4.69−4.14 (4H, m), 3.00−2.73 (1H, m), 2.37−1.89 (2H, m), 1.56−1.10 (22H, m), 0.87 (3H, t, J = 5.92); ^{13}C NMR (26 MHz, $CDCl_3$) δ (ppm) 174.63 (s), 153.76 (s), 89.56 (s), 74.62 (s), 66.07 (t), 49.47 (t), 31.88 (t), 30.39 (t), 29.60 (t) x 6, 29.02 (t) x 2, 27.65 (t), 22.63 (t), 18.59 (t), 14.03 (q). HRSMS-APCI (m/z): $[M + H]^+$ calcd for $C_{20}H_{34}O_3N$ 336.2533, found 336.2535.

Microorganisms. *Chromobacterium violaceum Bergonzini* (ATCC 12472) was purchased from the American Type Culture Collection (Manassas, VA, USA). Stock cultures were kept on trypticase soy agar (TSA, B.D. Diagnostic, Lenexa, KS). Inoculation of a single colony in 5 mL of Trypticase Soy Broth (TSB, B.D. Diagnostic Systems, Franklin Lakes, NJ) was achieved to prepare suspension cultures that were incubated and shaken for 18−20 h at 30 °C at 180 rpm. Before the susceptibility test experiments, bacteria cells were resuspended in TSB and visually standardized using 0.5 McFarland standard solution to provide an equivalent concentration of 1.0 × 10^8 colony-forming units (CFU)/mL.

Susceptibility Testing. Susceptibility tests were performed using routine procedures reported by Sanabria-Ríos' research group.[28,29,31,32] Briefly, stock solutions of HSLs **2**−**4** were prepared using 100% DMSO and serially diluted with sterile TSB supplemented with C6-HSL to final dilutions of 1, 0.5, and 0.25 mg/mL. 100 μL of each dilution was transferred to flat-bottomed microplate wells previously inoculated with 10 μL of TSB supplemented with C6-HSL solution containing (4−5) × 10^5 CFU. Each well was inspected spectrophotometrically at 600 nm using a control with no drug (containing the bacterial inoculated TSB with the 1% DMSO vehicle) and a quality control well (having sterile TSB without *N*-acyl-HSL solution) for further comparisons. The minimum inhibitory concentration (MIC) was the concentration at which the test compound prevented turbidity in the well after incubation for 18−20 h at 30 °C. The percentage of planktonic bacterial cell proliferation was calculated using eq 1.

$$\%\text{proliferation} = \left(\frac{\text{test compound sample OD at 600 nm}}{\text{OD of 1\% DMSO sample at 600 nm}}\right) \times 100 \quad (1)$$

Quantification of Violacein. The effect of HSLs **2**−**4** on violacein production in *C. violaceum* was measured by spectrophotometry at final concentrations of 1, 0.5, and 0.25 mg/mL, as described in the literature.[8,33,34] Briefly, *C. violaceum* was grown for 18−20 h until reaching approximately 1 × 10^8 CFU/mL. This bacterial culture was standardized using the 0.5 McFarland solution until equivalent turbidity was reached. A 25 mL sterile solution of TSB supplemented with C6-HSL was inoculated with 750 μL of the standardized *C. violaceum* solution. The resulting bacterial solution was used to inoculate TSB solutions containing either test compounds or 1% DMSO (vehicle) and incubated for 18−20 h at 30 °C. After incubation, bacterial pellets were resuspended with 2 mL of DMSO to dissolve the violacein produced by *C. violaceum*. All tubes were vigorously vortexed to extract the violacein pigment effectively. The *C. violaceum* debris was removed by centrifuging te sample at 5000 rpm for 5 min at room temperature, and the absorbance of soluble violacein was spectrophotometrically measured at 585 nm in a Varioskan

https://doi.org/10.1021/acsomega.4c01121
ACS Omega 2024, 9, 32536−32546

LUX multimode microplate reader (Thermo Scientific). The violacein production was calculated using an algorithm similar to eq 1 at 585 nm.

Quantification of Acyl-Homoserine Lactones (AHLs). As previously described, liquid−liquid extraction of AHLs was performed by spectrophotometry.[34,35] Briefly, 100 μL of TSB medium supplemented with 1% (w/v) glucose was inoculated with 10 μL of (4−5) × 10^5 CFU of *C. violaceum*. The resulting bacteria suspensions were dose-dependently loaded with 0.5 and 0.25 mg/mL HSL **4** in microplate wells and incubated at 30 °C for 18−20 h. This experimental design included *C. violaceum* treated with 1% DMSO as vehicle control with no drug. Then, bacterial cells were resuspended in the microplate and transferred to fresh centrifuge tubes. An equivalent volume of acidified ethyl acetate (0.5%, glacial acetic acid) was added, and the tubes were mixed well. The organic layers of both treated and control tubes were separated, and the organic solvent was removed by rotary evaporation and freeze-dried using a benchtop freeze-dryer (MillRock Technology, NY, USA). Subsequently, lyophilized samples (control and treated) were resuspended in 20% (v/v) acidified ethyl acetate and stored at −20 °C. Finally, in a microplate, wells were loaded with an equal mixture of 10% (w/v) of ferric chloride (4 M HCl) and 95% (v/v). Equation 1 was also used to calculated the percentage of AHL production at 520 nm.

MTT Approach to Determine Biofilm Inhibition. The MTT [3-(4,5-dimethylthiazol-2-yl)-2,5-diphenyltetrazolium bromide] approach was used to assess the effect of HSL **4** on *C. violaceum* biofilm formation as described in the literature.[36] Briefly, 100 μL of TSB medium supplemented with 1% (w/v) glucose was inoculated with 10 μL of (4−5) × 10^5 CFU of *C. violaceum*. The resulting bacterial suspensions were dose-dependently loaded with 1, 0.5, and 0.25 mg/mL HSL **4** in microplate wells and incubated at 30 °C for 20 h. After being washed with 1X PBS to remove the planktonic cells, the surface-adherent biofilm was treated with 100 μL of 1% (w/v) MTT-1X PBS solution and incubated for 2 h at 30 °C. After incubation, the MTT solution was removed from each well, and the bacterial biofilm was resuspended with 100 μL of DMSO. The microplate wells containing DMSO were incubated for 15 min at room temperature. The purple intensity of viable *C. violaceum* reducing tetrazolium to formazan was determined by measuring the OD at 570 nm with a Varioskan LUX multimode microplate reader (Thermo Scientific) at different treatment concentrations. Equation 1 allowed the calculation of the percentage of viable *C. violaceum* in a biofilm at 570 nm.

Visualization of *C. violaceum* Biofilm Using Fluorescence Microscopy. The light microscopic analysis method described for biofilm formation on glass coverslips was performed as previously described with some modifications.[37] Briefly, TSB media (supplemented with 0.2% (w/v) glucose) containing 0.25, 0.5, and 1 mg/mL HSL **4** and the corresponding 1% DMSO control vehicle were inoculated with 10 μL of (4−5) × 10^5 CFU of *C. violaceum* and incubated at 30 °C for 20 h on glass coverslips that were placed and covered with Petri dishes. After incubation, the free planktonic cells from treated and untreated coverslips were removed with distilled water, and adherent cells were stained with 0.2% crystal violet. The excess crystal violet was removed by washing twice with sterile distilled water, and the stained glass coverslips with the biofilm were visualized under a light microscope (MOTIC AE31E, Germany).

Cytotoxicity Evaluation Against Vero Cells Using the MTT Approach. Vero cells ATCC CCL-81.5 (Kidney African Green Monkey, Manassas, VA, USA) were cultured in DMEM (ATCC, Manassas, VA, USA) supplemented with 10% FBS (Hyclone, Waltham, MA, USA). Vero cells, with a final concentration of 2.5 × 10^4 cells/mL (5000 cells/well), were seeded on a 96-well plate (0.2 mL/well) and incubated for 24 h at 37 °C in a 5% CO_2 atmosphere. After 24 h, cells were treated with HSL **4** at concentrations ranging from 0.0039 to 1 mg/mL. Controls containing 1% DMSO were included in the experimental design for all assays. After incubation, the medium containing the test compound was removed. Adherent cells were washed with 100 μL of PBS 1X (Hyclone, GE Healthcare Life Sciences, UT, USA), then 0.5% (w/v) MTT solution (BeanTown Chemical, New Hampshire, USA) was added to each well (0.1 mL/well), and the samples were incubated for 2 h at 37 °C in a 5% CO_2 atmosphere. Subsequently, the MTT solution was removed, and cells containing formazan crystals were resuspended with DMSO (0.1 mL/well) and incubated for 15 min at 37 °C in a 5% CO_2 atmosphere. The purple intensity of viable Vero Cells reducing tetrazolium to formazan was quantified at 570 nm in a Varioskan LUX multimode microplate reader (Thermo Scientific). Experiments evaluating cytotoxic activity were conducted in three biological replicates (N = 3). Equation 1 was also used to calculate cell proliferation at 570 nm.

Molecular Docking Studies of CviR and Novel Acyl HSLs. Molecular docking studies were performed using Schrödinger Maestro software, version 13.5. CviR protein (PDB ID 3QP5) was retrieved from the Protein Data Bank (PDB). In the crystal structure, missing residues were added, and water molecules around the receptor binding site were removed using the Protein Preparation Workflow from Maestro. A receptor grid was generated using the cocrystallized ligand in 3QP5 before docking with Glide. A grid file was obtained to dock all the compounds of interest to the protein's binding pocket and generate the docking scores.

Ligand Preparation. Ligand preparation for the docking experiments was carried out by taking the PDB structures of the compounds and processing them using the LigPrep tool of Schrodinger suite 2023−2024 (Schrodinger, LLC, New York, NY). The compounds were optimized through the OPLS4 force field algorithm for energy minimization. This preparation resulted in all the ligand structures used for docking the target protein.

Procedure for Validating Molecular Docking Results. The Schrodinger suit was used to validate the docking results. This was done by extracting the cocrystallized ligand, chlorolactone (CL), from the binding pocket of the target protein (3QP5)[17] and then redocking it into the same binding site of the protein. The redocked ligand was superimposed on the initial structure, and the RMSD value was determined.

Statistical Analysis. One-way ANOVA followed by Tukey's test ($P < 0.05$) was conducted to determine statistical differences in *C. violaceum* proliferation, violacein production, AHL generation, biofilm formation, and Vero cell proliferation measurements. All the biostatistical analyses were performed in triplicate using GraphPad Prism 8.3.0 software (GraphPad Software Inc., La Jolla, CA, USA).

RESULTS

Synthesis of Novel Acyl HSLs. The synthesis of novel acyl HSL was performed as outlined in Schemes 1−3 to test

https://doi.org/10.1021/acsomega.4c01121
ACS Omega 2024, 9, 32536−32546

Scheme 1. Total Synthesis of Acyl HSLs 1 and 2

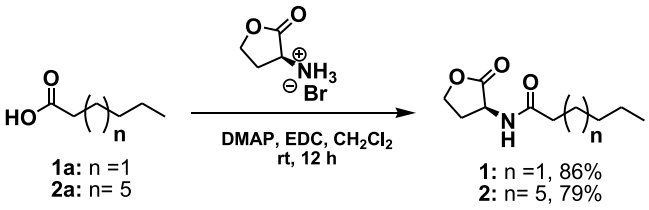

Scheme 3. Total Synthesis of the Novel Acyl HSL4

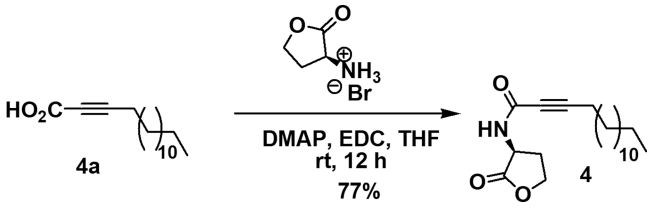

the anti-QS and other biological properties, such as biofilm formation, violacein and HSL production, and cytotoxicity in Vero cells. Scheme 1 shows the synthesis of C6-HSL and C10-HSL, performed in one step, where either **1a** or **2a** was reacted with commercially available HSL in the presence of DMAP and EDC in DCM at room temperature. HSLs **1** and **2** were obtained in 86% and 79% yields, respectively. Spectral data coincided with what was reported in the literature.[23,30]

The novel acyl HSL **3** was synthesized as displayed in Scheme 2. In this synthesis, alkynol **3a** was protected with DHP in PTSA catalytic conditions, followed by an acetylenic coupling reaction using *n*-BuLi in dry THF combined with 1,3-dimethyl-2-imidazolidinone (DMI), and finally removal of the tetrahydropyranyl protective group in methanolic-acidic conditions, which afforded alkynol **3b** in 73% yield. Alkynol **3b** was oxidized with PDC in DMF to obtain **3c** in 88% yield. Finally, compound **3** was prepared with a 59% yield by reacting **3c** with HSL in the presence of DMAP, EDC, and DCM.

In Scheme 3, we show the synthetic strategy for obtaining the novel acyl HSL **4**. For this synthetic strategy, **4a** was prepared as described by Sanabria-Rios et al.[28,29,31] Compound **4a** was treated with HSL and EDC catalyzed with DMAP in THF, yielding HSL **4** in 77% yield. The chemical identities of the novel HSL **3** and HSL **4** and their synthetic intermediates were confirmed by melting point determination, GC-MS, ^{1}H NMR, ^{13}C NMR, FT-IR, and HRMS analyses (see Material and Methods). HSLs **3** and **4** were confirmed as novel compounds through a literature search on SciFinder, a research discovery tool provided by the American Chemical Society (ACS).[38] Spectroscopic data for the novel final products HSL **3** and HSL **4** are available in the Supporting Information (SI).

Effect of *N*-Acyl HSL on the Growth and QS-Mediated Virulence Factors in *C. violaceum*. Once the syntheses of HSL **2**−**4** were carried out, their cytotoxic and anti-QS effects on *C. violaceum* (ATCC 12472) were determined at 0.25, 0.50, and 1 mg/mL (Figure 2). In this experimental approach, planktonic *C. violaceum* was quantified by measuring the bacterial turbidity at 600 nm. It can be observed from Figure 2 that C10-HSL was not toxic at the concentrations tested. In the case of HSL **3**, this compound showed cytotoxicity at 0.25, 0.50, and 1 mg/mL ($p < 0.5$), while HSL **4** was toxic at 1 mg/mL when compared with 1% DMSO as the control with no drug.

Figure 2 also shows the promising anti-QS activity of the novel *N*-acyl HSL at the sub-MIC level in a dose−response manner. Anti-QS activity was determined based on the violacein production by *C. violaceum*, which can be spectrophotometrically quantified at 585 nm. Results from Figure 2 show that *C. violaceum*, in the presence of C10-HSL, overproduces violacein, obtaining a 3-fold higher percentage value at 0.25 mg/mL than the corresponding 1% DMSO control with no drug, where a significant difference was observed ($p < 0.5$) after biostatistical analysis using one-way ANOVA. However, at 1 mg/mL, C10-HSL significantly inhibits violacein production, demonstrating anti-QS activity at that concentration. In the case of HSL **3**, this compound inhibited violacein production at 0.25, 0.50, and 1 mg/mL. Furthermore, it can be observed from Figure 2 that the novel HSL **4** displayed significant inhibition of violacein production at 0.5 and 1 mg/mL, which strongly suggests that this *N*-acyl HSL affected QS in *C. violaceum*.

Inhibitory Effect of HSL 4 on the Generation of Acyl HSL in *C. violaceum*. Since compound, HSL **4** displayed significant anti-QS activity (see the complete spectroscopic characterization in the SI), we tested its ability to inhibit the generation of acyl HSL in *C. violaceum*. Acyl HSL in *C. violaceum* was quantified through liquid−liquid extractions followed by spectrophotometric analyses at 520 nm. Results from these tests are displayed in Figure 3. It can be observed that HSL **4** significantly inhibited the generation of acyl HSL at 0.5 and 1 mg/mL since the statistical difference was detected in one-way ANOVA when compared with 1% DMSO, the control with no drug.

Scheme 2. Total Synthesis of the Novel Acyl HSL 3

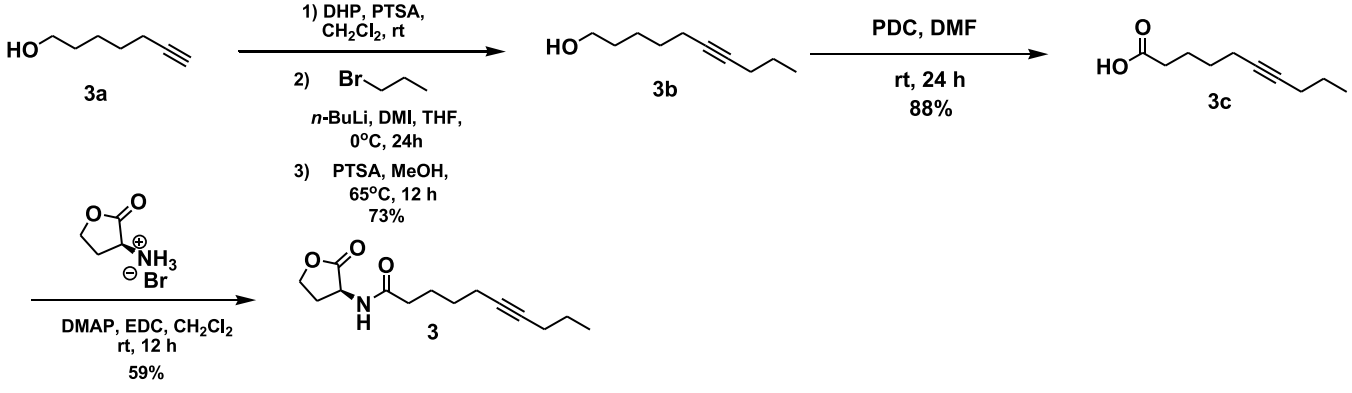

https://doi.org/10.1021/acsomega.4c01121
ACS Omega 2024, 9, 32536−32546

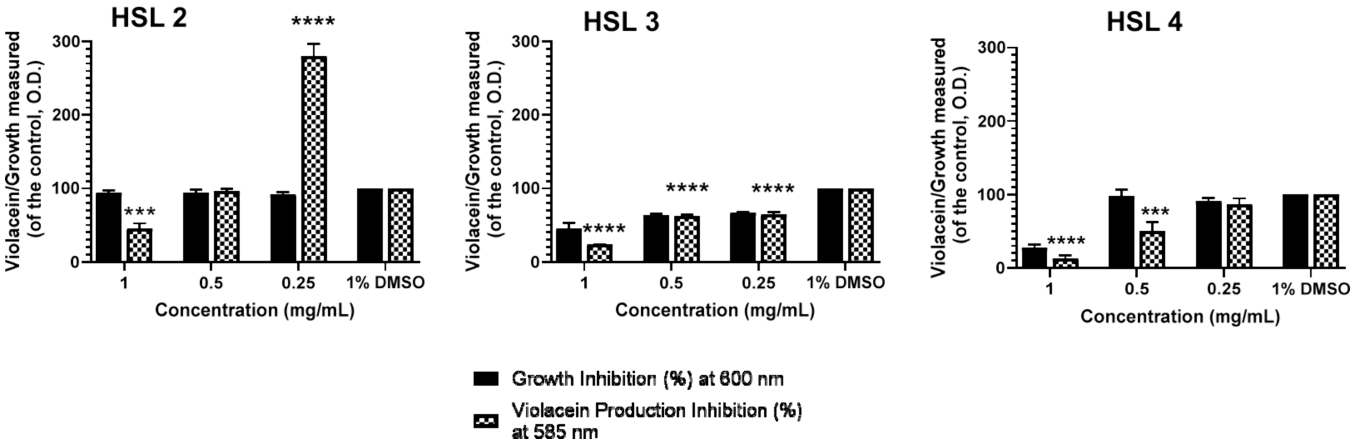

Figure 2. Bar graphs showing the effect of inhibitory and subinhibitory concentrations of acyl HSLs (1, 0.5, and 0.25 mg/mL) on *C. violaceum* viability and QS-mediated violacein production. Planktonic *C. violaceum* cells were quantified by measuring bacterial turbidity at 600 nm, while the quantitative assessment of violacein was performed at 585 nm. One-way ANOVA followed by Tukey's test revealed a statistical difference between averaged experimental samples and the corresponding negative control (1% DMSO) since $p < 0.05$ (*), $p < 0.01$ (**), $p < 0.001$ (***), and $p < 0.0001$ (****) were obtained. All experiments were performed in three biological replicates ($N = 3$).

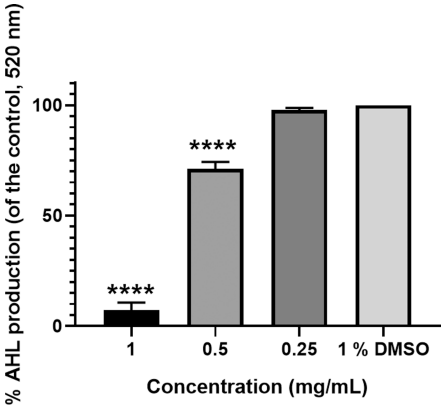

Figure 3. Bar graphs showing the effect of inhibitory and subinhibitory concentrations of HSL **4** (1, 0.5, and 0.25 mg/mL) on the generation of acyl HSLs in *C. violaceum*. Liquid−liquid extractions of AHLs were performed, and the samples were analyzed by spectrophotometry at 520 nm. One-way ANOVA followed by Tukey's test revealed a statistical difference between averaged experimental samples and the corresponding negative control (1% DMSO) since $p < 0.05$ (*), $p < 0.01$ (**), $p < 0.001$ (***), and $p < 0.0001$ (****) were obtained. All experiments were performed in three biological replicates ($N = 3$).

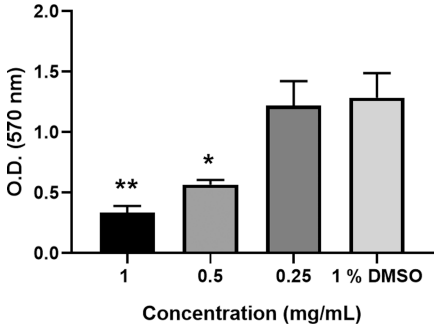

Figure 4. Bar graphs showing the effect of the inhibitory and subinhibitory concentrations of novel HSL **4** on the biofilm formation of *C. violaceum* (1, 0.5, and 0.25 mg/mL). Adherent bacterial cells were treated with 1% (w/v) 1X PBS-MTT solution, and the purple intensity of viable *C. violaceum*, reducing tetrazolium to formazan, was measured at 570 nm. One-way ANOVA followed by Tukey's test revealed a statistical difference between averaged experimental samples and the corresponding negative control (1% DMSO) since $p < 0.05$ (*), $p < 0.01$ (**), $p < 0.001$ (***), and $p < 0.0001$ (****) were obtained. All experiments were performed in three biological replicates ($N = 3$).

Effect of HSL 4 on the Biofilm Formation in *C. violaceum*. The effect of HSL **4** on biofilm formation was determined by exposing *C. violaceum* to subinhibitory concentrations of 1, 0.5, and 0.25 mg/mL the test compound (Figure 4). Planktonic *C. violaceum* cells were discarded, and adherent cells were treated with 1% (w/v) 1X PBS-MTT solution. Viable cells in the biofilm were quantified through spectrophotometric assessment of the purple intensity (indicative of bacterial metabolic activity due to the reduction of tetrazolium to formazan) at 570 nm. Results in Figure 4 show that HSL **4** inhibited biofilm formation at 0.5 and 1 mg/mL since significant statistical differences ($p < 0.5$) were observed between OD values of HSL **4**-treated bacteria and the 1% DMSO control with no drug.

In addition to the MTT approach, light microscopy analysis was performed *in situ* to determine the effect of HSL **4** on the biofilm formation in *C. violaceum*. Figure 5 shows representative images from light microscopy analysis when *C. violaceum* was treated with HSL **4** at subinhibitory concentrations of 0.25, 0.5, and 1 mg/mL. It can be noted from Figure 5 that bacterial aggregation was observed when *C. violaceum* was treated with either 1% DMSO or 0.25 mg/mL HSL **4**. However, when *C. violaceum* was treated with either 0.5 or 1 mg/mL HSL **4**, a drastic reduction in the biofilm cluster was observed compared to 1% DMSO.

Cytotoxic Effect of HSL 4 on the Proliferation of Vero Cells. The cytotoxic effect of HSL **4** on the proliferation of Vero cells (ATCC CCL-81.5) was assessed using the MTT approach after 24 h of incubation. Viable Vero cells were spectrophotometrically quantified by measuring the purple intensity at 570 nm associated with the reduction of tetrazolium to formazan. Results from MTT experiments are displayed in Figure 6. Results in Figure 6 demonstrate that HSL **4** is not toxic in concentrations ranging from 0.0039 to 1 mg/mL. One-way ANOVA did not detect significant differ-

https://doi.org/10.1021/acsomega.4c01121
ACS Omega 2024, 9, 32536−32546

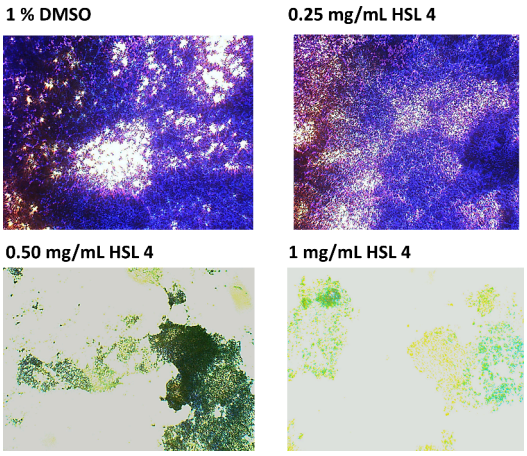

Figure 5. Representative images obtained from the *in situ* light microscopy analysis of the antibiofilm activity of HSL **4** in *C. violaceum*. Bacteria treated with 1% DMSO represent the control of the microscopy experiments. The control sample containing 1% DMSO displays biofilm formation after 20 h of exposure to HSL **4**, while 0.5 mg/mL HSL **4** significantly decreases biofilm formation after 20 h. A cytotic effect was observed when *C. violaceum* was treated with HSL **4** at 1 mg/mL. All experiments were performed in three biological replicates (N = 3).

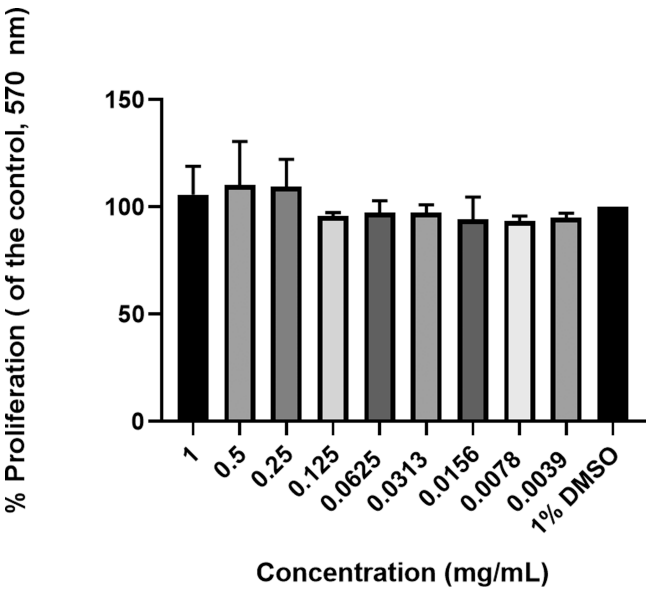

Figure 6. Bar graphs showing the cytotoxic effect of HSL **4** on the proliferation of Vero Cells (ATCC CCL-81.5). Vero cells were treated with HSL **4** at concentrations ranging from 0.0039 to 1 mg/mL. 1% MTT-1X PBS solution was added to cells after 24 h of incubation, and the purple intensity of viable cells, reducing tetrazolium to formazan, was measured at 570 nm. Experiments were performed in three biological replicates (N = 3). One-way ANOVA followed by Tukey's test revealed no statistical difference between averaged experimental samples and the corresponding negative control (1% DMSO) since $p > 0.05$ was obtained.

ences ($p > 0.5$) between HSL **4**-treated and 1% DMSO-treated *C. violaceum* (control with no drug).

Molecular Docking Analysis. The CviR gene plays a critical role in controlling QS, biofilm formation, and other mechanisms related to the subsistence of *C. violaceum*.[39] HSL **4** was subjected to docking studies and docking score prediction using the CviR receptor protein. Molecular docking studies were performed using the CviR protein (PDB ID 3QP5) retrieved from the RCSB Protein Data Bank.[40] To validate our molecular docking results, we used the crystal structure of the CviR protein and its cocrystallized ligand, CL.[17] We carried out separate redocking experiments for the protein and the ligand. Upon analysis, we found a root-mean-square deviation (RMSD) value of 1.4802 Å, which is considered within the acceptable range for a good match between predicted and crystallographic structures (*i.e.*, <2.0 Å).[41] Our study has revealed that among the three analogs of C10-HSL, HSL **4** shows the best interaction with the active site of CviR. Specifically, our molecular docking results indicate that the docking score of HSL **4** with the active site of CviR is −5.71 kcal/mol. In contrast, the corresponding C10-HSL (**2**) and HSL **3** scores are −2.61 and −3.69 kcal/mol, respectively. The study compares the interactions of CL and HSL **4** compounds at the active site of CviR (PDB ID 3QP5, Figure 7), highlighting their polar and hydrophobic interactions with amino acids and showing the unique binding features with specific amino acids not observed in CL. In addition, the schematic 3D representation of HSL **4** (Figure 8) shows hydrogen bonding between HSL **4** and Leu 72 and between HSL **4** and Gln 95, which can explain the docking score of HSL **4** when interacting with the CviR binding pocket.

DISCUSSION

Novel *N*-acyl HSLs were synthesized to investigate their effect on QS-controlled mechanisms that confer resistance to *C. violaceum*, such as biofilm, violacein, and HSL production. In addition, the potential of novel HSLs as "nontraditional" antibiotics was assessed by performing the MTT approach, which allowed the determination of the cytotoxic effect of these HSLs on the proliferation of Vero cells. For this study, the term "nontraditional antibiotic" will be used when the mechanism of action of a particular antibiotic affects bacterial resistance mechanisms in bacteria without necessarily killing the microorganism.[42] This work is the first report providing evidence that previously synthesized 2-alkynoic antibacterial fatty acids can be used as starting materials for the synthesis of novel analogs of C6-HSL (Figure 1) with the potential to inhibit QS-mediated mechanisms.[28,29,31,32]

In this study, we synthesized three HSLs using synthetic strategies described in Schemes 1−3. Once these compounds were synthesized, the effect of HSL on bacterial cell growth and violacein production was investigated (Figure 2). Results in Figure 2 show that C10-HSL was not bactericidal against *C. violaceum*, while HSLs **3** and **4** displayed an antibacterial effect on the growth of *C. violaceum*. HSL **3** was bactericidal against *C. violaceum* at 0.25, 0.50, and 1 mg/mL. However, HSL **4** only displayed bacterial cytotoxicity at 1 mg/mL. The findings in Figure 2 show the following trend regarding the antibacterial activity of the synthesized *N*-acyl HSLs: HSL **3** > HSL **4** > C10-HSL. In terms of chemical structures, it can be observed that the presence of a triple bond drastically changed the antibacterial properties of HSLs (see Figure 2). The effect of incorporating a triple bond at C-6 in the acyl moiety of an HSL is remarkable when the antibacterial activities of C10-HSL and HSL **3** against *C. violaceum* are compared. In addition, the results in Figure 2 confirm that a triple bond at C-2 in the acyl moiety of HSL **4** and a C-16 chain length have important roles in both antibacterial and anti-QS properties against *C. violaceum*, which is consistent with previous findings reported

https://doi.org/10.1021/acsomega.4c01121
ACS Omega 2024, 9, 32536−32546

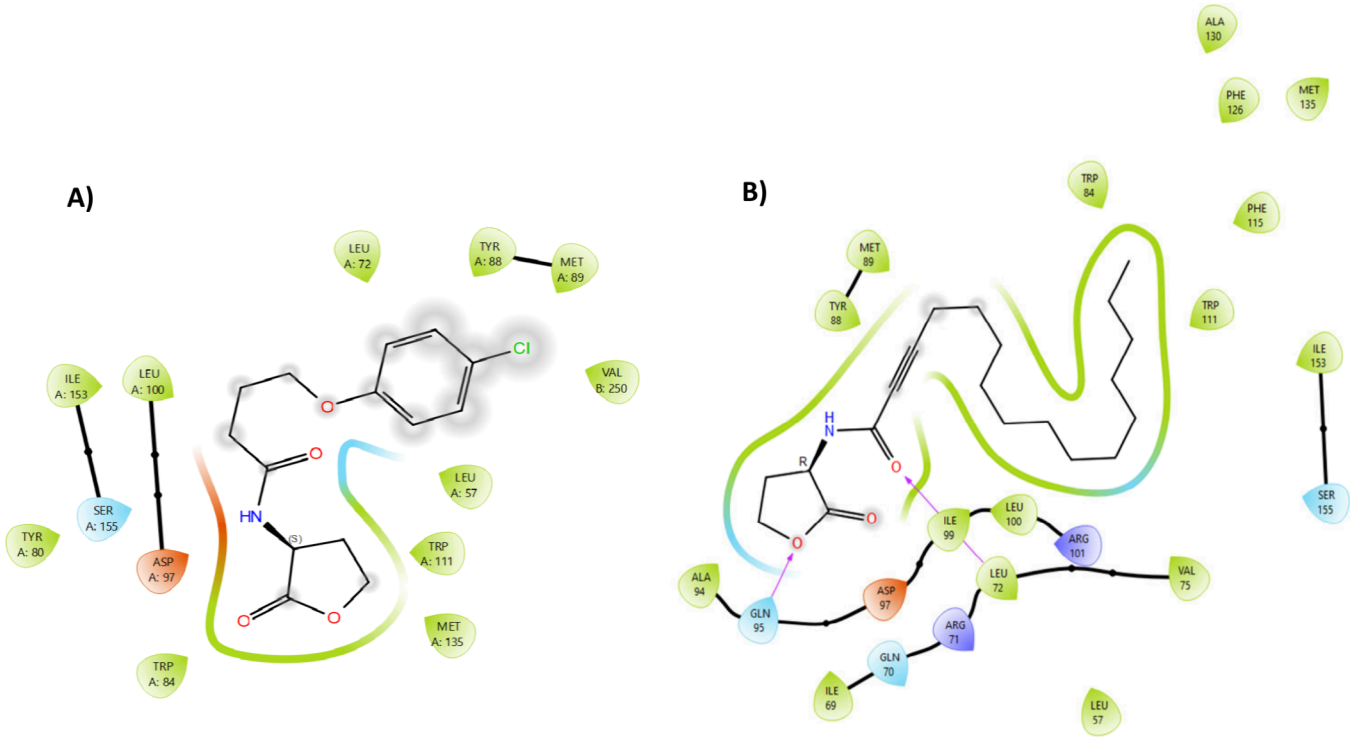

Figure 7. Schematic 2D molecular interactions between the CviR active site and either (A) the CL cocrystal ligand or (B) the novel HSL **4**. Light blue and green colors represent polar and hydrophobic interactions, respectively, while purple arrows identify hydrogen bonding. The colors red and purple represent negatively and positively charged amino acids, respectively.

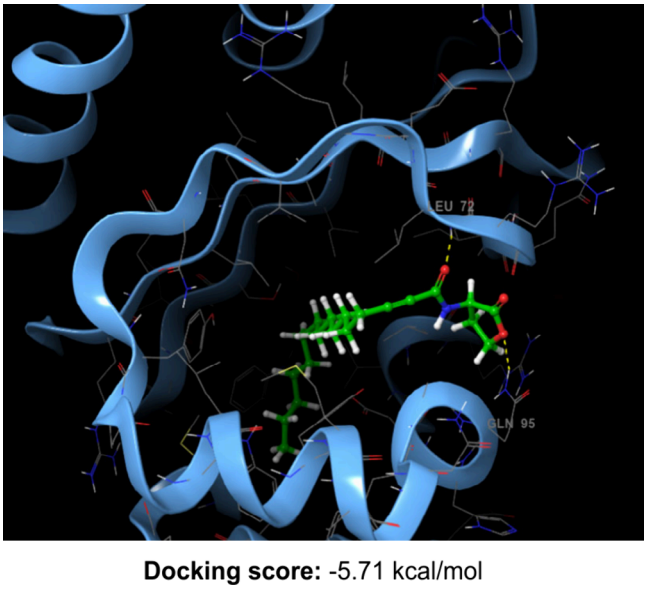

Figure 8. Schematic 3D image showing the interaction between HSL **4** and CviR. Dashed yellow lines represent hydrogen bonding between HSL **4** and Leu 72 or Gln 95.

in the literature regarding antibacterial unsaturated fatty acids.[28,29]

Figure 2 also demonstrates that C10-HSL promotes the overproduction of violacein at 0.25 mg/mL of the test compound in TSB supplemented with C6-HSL. Desvecovi et al. reported that the overproduction of violacein in *C. violaceum* occurs when negative regulation of the CviR/R QS system occurs.[43] Thus, this alternative regulation of the CviR/R QS system likely occurred when *C. violaceum* was exposed to C10-HSL combined with C6-HSL. In addition, it was observed that C10-HSL inhibited violacein generation at 1 mg/mL; this finding is consistent with those reported in the literature regarding the anti-QS properties of C10-HSL.[23] It is important to emphasize that HSL **3** does not necessarily inhibit violacein production by interfering with the CviR/R QS system. This compound probably inhibits violacein production by inhibiting the growth of *C. violaceum*, as shown in Figure 2. In the case of HSL **4**, the inhibitory effect of this compound on violacein production at 1 mg/mL can also be attributed to its antibacterial activity against *C. violaceum* (see Figure 2). It is important to note in Figure 2 that HSL **4** is not antibacterial against *C. violaceum* at the subinhibitory concentrations of 0.25 and 0.50 mg/mL. Indeed, the latter compound was the most active inhibitor of violacein production at 0.50 mg/mL when compared with the other HSLs tested. For this reason, HSL **4** was selected as the test compound for the other experiments presented herein.

In *C. violaceum* QS, CviI synthesizes acyl-HSLs, while CviR is a transcription factor that binds to DNA in the cytoplasm and promotes gene expression after binding to acyl-HSLs.[44] Therefore, the production of HSL by *C. violaceum* is critical for bacterial QS and needs further investigation. As shown in Figure 2, HSL **4** inhibited violacein production at the subinhibitory concentration of 0.50 mg/mL. Because violacein production is a QS-dependent mechanism,[7] it was hypothesized that HSL **4** could affect the acyl-HSL production in *C. violaceum*. To test this hypothesis, liquid−liquid extractions were performed to determine the effect of HSL **4** on acyl-HSL production in *C. violaceum* (Figure 3). When results in Figures 2 and 3 are analyzed, a correlation between violacein and acyl-HSL production is observed. For example, at 0.5 mg/mL, HSL **4** inactivated the violacein production, possibly by inhibiting

https://doi.org/10.1021/acsomega.4c01121
ACS Omega 2024, 9, 32536−32546

the HSL production. Alternatively, the HSL production decreases at 1 mg/mL because *C. violaceum* is susceptible to HSL **4** at that concentration.

It is known that the QS system coordinates and regulates the biofilm architecture in a wide variety of Gram-negative bacterial pathogens associated with human infections.[45] For this reason, the MTT approach and light microscopic analyses were performed to determine the effect of HSL **4** on the biofilm formation in *C. violaceum* (Figures 4 and 5) and establish whether this effect can be associated with its anti-QS activity (Figure 2). Data in Figure 4 demonstrate that HSL **4** inhibited biofilm formation in *C. violaceum* at the subinhibitory concentration of 0.5 mg/mL, implying that HSL **4**, when affecting bacterial QS, also affects the ability of the bacteria to form biofilms. Results in Figure 4 are supported by images presented in Figure 5, where a drastic biofilm reduction was observed when *C. violaceum* was exposed to 0.5 mg/mL of the test compound. The present data agree with Venkatramanan et al.'s findings, who reported the reduction of biofilm formation in biofilm inhibitory assays and light microscopic analysis when *C. violaceum* was exposed to fruit extracts of *Passiflora edulis*.[34] Figures 4 and 5 also show the effect of the antibacterial activity of HSL **4** in *C. violaceum* at 1 mg/mL and its influence on bacterial biofilm formation.

Another aspect that needs to be discussed is the potential of HSLs as "nontraditional" antibiotics. In this study, the cytotoxic effect of HSL **4** on the proliferation of Vero cells was assessed to determine the selectivity of this compound as a "nontraditional" antibiotic. Figure 6 shows that HSL **4** is not toxic toward Vero Cells since inhibition of cell proliferation was not observed at concentrations ranging from 1 to 0.0039 mg/mL, demonstrating its potential as a "nontraditional" antibiotic in further investigations.

Figure 7 shows how CL and HSL **4** interact with CviR's active site (PDB ID 3QP5), showing the similarities and differences in these interactions. Both compounds have polar interactions with Ser 155 and interact with the negatively charged Asp 97. CL and HSL **4** also display hydrophobic interactions with Trp 111 and Leu 100, indicating similar binding modes and affinities within the active site of CviR. However, only HSL **4** exhibits polar interactions with Gln 95 and Gln 70 and electrostatic interactions with positively charged residues Arg 71 and Arg 101 when binding with CviR. Furthermore, it was identified that HSL **4** displayed a binding score of −5.71 kcal/mol (Figure 8). In comparison, C10-HSL and HSL **3** displayed binding scores of −2.61 and −3.69 kcal/mol, respectively, suggesting that HSL **4** interacts with the CviR active site better than C10-HSL or HSL **3**. The binding scores obtained from *in silico* studies strongly support the structure−activity relationship (SAR) results displayed in Figure 2, which demonstrated the effectiveness of HSL **4** as an anti-QS agent. Moreover, molecular docking results also identify hydrogen bonding interactions between HSL **4** and Leu 72 and between HSL **4** and Gln 95, suggesting the importance of Leu 72 and Gln 95 in suppressing the QS system activity in *C. violaceum*.

CONCLUSIONS

The total synthesis of novel acetylenic HSLs was performed, and their activities as inhibitors of QS activity and other QS-dependent mechanisms were tested. Among the three HSLs synthesized, HSL **4** is the most promising candidate for investigating its antipathogenic effect. Results from this study suggest that HSL **4** potentially interferes with AHL-based QS-controlled virulence factors and biofilm formation in *C. violaceum*. Docking scores revealed that HSL **4** binds to the CviR receptor, suggesting that this compound can disrupt QS activity and other related mechanisms by interacting with this receptor. Additionally, it was found that HSL **4** is not toxic to Vero cells, demonstrating its selectivity to *C. violaceum* QS. However, it is important to acknowledge that further investigation is needed to broaden bacterial strains that use QS to resist antibiotics and explore other cell lines to assess cytotoxicity in normal eukaryotic cells. The findings generated from this study highlight the anti-QS and biofilm potential of novel acetylenic HSLs for further studies for pharmacological and real-time therapeutic applications.

ASSOCIATED CONTENT

Supporting Information

The Supporting Information is available free of charge at https://pubs.acs.org/doi/10.1021/acsomega.4c01121.

Comprehensive spectroscopic data (FT-IR, ^{1}H NMR, ^{13}C NMR, and APCI mass spectrometry) and molecular docking validation (PDF)

AUTHOR INFORMATION

Corresponding Author

David J. Sanabria-Ríos − *Faculty of Science and Technology, Inter American University of Puerto Rico, San Juan, Puerto Rico 00919, United States; Medicinal Research and Applications Laboratory, Inter American University of Puerto Rico, San Juan, Puerto Rico 00919, United States;* orcid.org/0000-0001-8797-1210; Phone: 787-250-1912; Email: dsanabria@intermetro.edu; Fax: 787-250-8736

Authors

Rene García-Del-Valle − *Department of Chemistry, University of Puerto Rico, San Juan, Puerto Rico 00925, United States*

Sachel Bosh-Fonseca − *Faculty of Science and Technology, Inter American University of Puerto Rico, San Juan, Puerto Rico 00919, United States*

Joangely González-Pagán − *Faculty of Science and Technology, Inter American University of Puerto Rico, San Juan, Puerto Rico 00919, United States*

Alanis Díaz-Rosa − *Faculty of Science and Technology, Inter American University of Puerto Rico, San Juan, Puerto Rico 00919, United States*

Karina Acevedo-Rosario − *Faculty of Science and Technology, Inter American University of Puerto Rico, San Juan, Puerto Rico 00919, United States*

Luzmarie Reyes-Vicente − *Faculty of Science and Technology, Inter American University of Puerto Rico, San Juan, Puerto Rico 00919, United States; Medicinal Research and Applications Laboratory, Inter American University of Puerto Rico, San Juan, Puerto Rico 00919, United States*

Antonio Colom − *Faculty of Science and Technology, Inter American University of Puerto Rico, San Juan, Puerto Rico 00919, United States*

Néstor M. Carballeira − *Department of Chemistry, University of Puerto Rico, San Juan, Puerto Rico 00925, United States*

Complete contact information is available at: https://pubs.acs.org/10.1021/acsomega.4c01121

https://doi.org/10.1021/acsomega.4c01121
ACS Omega 2024, 9, 32536−32546

Notes

The authors declare no competing financial interest.

■ ACKNOWLEDGMENTS

This project was supported by the National Center for Research Resources and the National Institute of General Medical Sciences of the National Institutes of Health through Grant P20GM103475-21. Dr. D. J. Sanabria-Ríos would like to thank the Inter American University of Puerto Rico-Metropolitan Campus (IAUPR-MC) for sponsoring part of this project. J.G.-P., A.D.-R., and K.A.-R. acknowledge the support of the IAUPR-MC-Title V Active Learning Center of Excellence (ALCE) Program (P031S200066) and the STEM-Guided Pathway Approach (P031C210037) for the stipend to conduct this project. R.G.d.V. thanks the UPR-Río Piedras NIH-NIGMS RISE program (award number 5R25GM061151-22) for an undergraduate fellowship. D.J.S.-R. also thanks Dr. Frederick Strobel (Emory University) for performing HRMS analyses.

■ REFERENCES

(1) Kumar, M. R. *Chromobacterium violaceum*: A rare bacterium isolated from a wound over the scalp. *Int. J. Appl. Basic. Med. Res.* **2012**, *2* (1), 70.

(2) Alisjahbana, B.; Debora, J.; Susandi, E.; Darmawan, G. *Chromobacterium violaceum*: A review of an unexpected scourge. *Int. J. Gen. Med.* **2021**, *14*, 3259.

(3) Frawley, A. A.; Powell, L.; McQuiston, J. R.; Gulvik, C. A.; Bégué, R. E. Necrotizing pneumonia caused by *Chromobacterium violaceum*: Report of a rare human pathogen causing disease in an Immunodeficient child. *Am. J. Trop. Med. Hyg.* **2018**, *99* (1), 164.

(4) Kothari, V.; Sharma, S.; Padia, D. Recent research advances on *Chromobacterium violaceum*. *Asian Pac. J. Trop. Med.* **2017**, *10* (8), 744.

(5) Durán, N.; Justo, G. Z.; Durán, M.; Brocchi, M.; Cordi, L.; Tasic, L.; Castro, G. R.; Nakazato, G. Advances in *Chromobacterium violaceum* and properties of violacein-Its main secondary metabolite: A review. *Biotechnol. Adv.* **2016**, *34* (5), 1030.

(6) Fazal, A.; Yang, M.; Wang, M.; Ali, F.; Wen, Z.; Yin, T.; Zhao, X.; Hua, X.; Han, H.; Lin, H.; Wang, X.; Lu, G. H.; qi, J.; Yang, Y. Assessment of shikonin and acetyl-shikonin for mitigating quorum sensing potential of *C. violaceum*. *Plant Growth Regul.* **2021**, *94*, 233.

(7) McClean, K. H.; Winson, M. K.; Fish, L.; Taylor, A.; Chhabra, S. R.; Camara, M.; Daykin, M.; Lamb, J. H.; Swift, S.; Bycroft, B. W.; Stewart, G.; Williams, P. Quorum sensing and *Chromobacterium violaceum*: Exploitation of violacein production and inhibition for the detection of *N*-acylhomoserine lactones. *Microbiology* **1997**, *143*, 3703.

(8) Blosser, R. S.; Gray, K. M. Extraction of violacein from *Chromobacterium violaceum* provides a new quantitative bioassay for *N*-acyl homoserine lactone autoinducers. *J. Microbiol. Methods* **2000**, *40* (1), 47.

(9) Martinelli, D.; Grossmann, G.; Séquin, U.; Brandl, H.; Bachofen, R. Effects of natural and chemically synthesized furanones on quorum sensing in *Chromobacterium violaceum*. *BMC Microbiol.* **2004**, *4*, 25.

(10) Morohoshi, T.; Fukamachi, K.; Kato, M.; Kato, N.; Ikeda, T. Regulation of the violacein biosynthetic gene cluster by acylhomoserine lactone-mediated quorum sensing in *Chromobacterium violaceum* ATCC 12472. *Biosci. Biotechnol. Biochem.* **2010**, *74* (10), 2116.

(11) Durán, M.; Faljoni-Alario, A.; Durán, N. *Chromobacterium violaceum* and its important metabolites-review. *Folia Microbiol.* **2010**, *55* (6), 535.

(12) Mion, S.; Carriot, N.; Lopez, J.; Plener, L.; Ortalo-Magné, A.; Chabrière, E.; Culioli, G.; Daudé, D. Disrupting quorum sensing alters social interactions in *Chromobacterium violaceum*. *NPJ. Biofilms Microbiomes* **2021**, *7* (1), 40.

(13) Miller, M. B.; Bassler, B. L. Quorum sensing in bacteria. *Annu. Rev. Microbiol.* **2001**, *55*, 165.

(14) Rutherford, S. T.; Bassler, B. L. Bacterial quorum sensing: Its role in virulence and possibilities for its control. *Cold Spring Harb. Perspect. Med.* **2012**, *2* (11), a012427.

(15) Castillo-Juárez, I.; Maeda, T.; Mandujano-Tinoco, E. A.; Tomás, M.; Pérez-Eretza, B.; García-Contreras, S. J.; Wood, T. K.; García-Contreras, R. Role of quorum sensing in bacterial infections. *World J. Clin. Cases* **2015**, *3* (7), 575.

(16) Morohoshi, T.; Kato, M.; Fukamachi, K.; Kato, N.; Ikeda, T. *N*-acylhomoserine lactone regulates violacein production in *Chromobacterium violaceum* type strain ATCC 12472. *FEMS Microbiol. Lett.* **2008**, *279* (1), 124.

(17) Chen, G.; Swem, L. R.; Swem, D. L.; Stauff, D. L.; O'Loughlin, C. T.; Jeffrey, P. D.; Bassler, B. L.; Hughson, F. M. A strategy for antagonizing quorum sensing. *Mol. Cell* **2011**, *42* (2), 199.

(18) Rasmussen, T. B.; Givskov, M. Quorum-sensing inhibitors as anti-pathogenic drugs. *Int. J. Med. Microbiol.* **2006**, *296* (2−3), 149.

(19) Ravichandran, V.; Zhong, L.; Wang, H.; Yu, G.; Zhang, Y.; Li, A. Virtual screening and biomolecular interactions of CviR-based quorum sensing inhibitors against *Chromobacterium violaceum*. *Front. Cell Infect. Microbiol.* **2018**, *8*, 292.

(20) Ibrahim, Y. M.; Abouwarda, A. M.; Omar, F. A. Effect of kitasamycin and nitrofurantoin at subinhibitory concentrations on quorum sensing regulated traits of *Chromobacterium violaceum*. *Antonie Van Leeuwenhoek* **2020**, *113* (11), 1601.

(21) Wang, W.; Lin, X.; Yang, H.; Huang, X.; Pan, L.; Wu, S.; Yang, C.; Zhang, L.; Li, Y. Anti-quorum sensing evaluation of methyl-eugenol, the principal bioactive component, from the *Melaleuca bracteata* leaf oil. *Front. Microbiol.* **2022**, *13*, 970520.

(22) Ikeda, T.; Kajiyama, K.; Kita, T.; Takiguchi, N.; Kuroda, A.; Kato, J.; Ohtake, H. The synthesis of optically pure enantiomers of *N*-acyl-homoserine lactone autoinducers and their analogues. *Chem. Lett.* **2001**, *30* (4), 314.

(23) Chhabra, S. R.; Harty, C.; Hooi, D. S.; Daykin, M.; Williams, P.; Telford, G.; Pritchard, D. I.; Bycroft, B. W. Synthetic analogues of the bacterial signal (quorum sensing) molecule *N*-(3-oxododecanoyl)-L-homoserine lactone as immune modulators. *J. Med. Chem.* **2003**, *46* (1), 97.

(24) Svirskaya, P. I.; Leznoff, C. C.; Weatherston, J.; Laing, J. E. Syntheses of trans alken-1-ols as candidates for insect sex attractants. *J. Chem. Eng. Data* **1979**, *24* (2), 152.

(25) Macaulay, S. R. The rearrangement of isomeric linear decyn-1-ols by reaction with the sodium salt of 1,3-diaminopropane. *Can. J. Chem.* **1980**, *58* (23), 2567.

(26) Streit, A. D.; Zoll, A. J.; Hoang, G. L.; Ellman, J. A. Annulation of Hydrazones and Alkynes via Rhodium(III)-Catalyzed Dual C-H Activation: Synthesis of Pyrrolopyridazines and Azolopyridazines. *Org. Lett.* **2020**, *22* (3), 1217.

(27) 6-Decynoic acid. *PubChem*. National Center for Biotechnology Information, n.d. https://pubchem.ncbi.nlm.nih.gov/compound/6-Decynoic-acid (accessed 2023-11-10).

(28) Sanabria-Ríos, D. J.; Rivera-Torres, Y.; Maldonado-Domínguez, G.; Domínguez, I.; Ríos, C.; Díaz, D.; Rodríguez, J. W.; Altieri-Rivera, J. S.; Ríos-Olivares, E.; Cintrón, G.; Montano, N.; Carballeira, N. M. Antibacterial activity of 2-alkynoic fatty acids against multidrug-resistant bacteria. *Chem. Phys. Lipids* **2014**, *178*, 84.

(29) Sanabria-Ríos, D. J.; Morales-Guzmán, C.; Mooney, J.; Medina, S.; Pereles-De-León, T.; Rivera-Román, A.; Ocasio-Malavé, C.; Díaz, D.; Chorna, N.; Carballeira, N. M. Antibacterial activity of hexadecynoic acid isomers toward clinical isolates of multidrug-resistant *Staphylococcus aureus*. *Lipids* **2020**, *55* (2), 101.

(30) Geske, G. D.; Wezeman, R. J.; Siegel, A. P.; Blackwell, H. E. Small molecule inhibitors of bacterial quorum sensing and biofilm formation. *J. Am. Chem. Soc.* **2005**, *127* (37), 12762.

(31) Sanabria-Ríos, D. J.; Rivera-Torres, Y.; Rosario, J.; Gutierrez, R.; Torres-García, Y.; Montano, N.; Ortíz-Soto, G.; Ríos-Olivares, E.; Rodríguez, J. W.; Carballeira, N. M. Chemical conjugation of 2-hexadecynoic acid to C5-curcumin enhances its antibacterial activity

https://doi.org/10.1021/acsomega.4c01121
ACS Omega 2024, 9, 32536−32546

against multi-drug resistant bacteria. *Bioorg. Med. Chem. Lett.* **2015**, *25* (22), 5067.
(32) Sanabria-Rios, D. J.; Alequin-Torres, D.; De Jesus, A.; Cortes, G.; Carballeira, N. M.; Jauregui-Matos, V. Vinyl halogenated fatty acids display antibacterial activity against clinical isolates of methicillin-resistant *Staphylococcus aureus*. *Med. Res. Arch.* **2022**, DOI: 10.18103/mra.v10i7.2901.
(33) Ganesh, P. S.; Rai, R. V. Attenuation of quorum-sensing-dependent virulence factors and biofilm formation by medicinal plants against antibiotic resistant *Pseudomonas aeruginosa*. *J. Tradit. Complement. Med.* **2018**, *8* (1), 170.
(34) Venkatramanan, M.; Ganesh, P. S.; Senthil, R.; Akshay, J.; Ravi, A. V.; Langeswaran, K.; Vadivelu, J.; Nagarajan, S.; Rajendran, K.; Shankar, E. M. Inhibition of quorum sensing and biofilm formation in Chromobacterium violaceum by fruit extracts of *Passiflora edulis*. *ACS Omega* **2020**, *5* (40), 25605.
(35) Taghadosi, R.; Shakibaie, M. R.; Masoumi, S. Biochemical detection of *N*-acyl homoserine lactone from biofilm-forming uropathogenic *Escherichia coli* isolated from urinary tract infection samples. *Rep. Biochem. Mol. Biol.* **2015**, *3* (2), 56.
(36) Tang, H. J.; Chen, C. C.; Cheng, K. C.; Toh, H. S.; Su, B. A.; Chiang, S. R.; Ko, W. C.; Chuang, Y. C. In vitro efficacy of fosfomycin-containing regimens against methicillin-resistant *Staphylococcus aureus* in biofilms. *J. Antimicrob. Chemother.* **2012**, *67* (4), 944.
(37) Gopu, V.; Shetty, P. H. Cyanidin inhibits quorum signalling pathway of a food borne opportunistic pathogen. *J. Food Sci. Technol.* **2016**, *53* (2), 968.
(38) CAS SciFinder. *Chemical Abstract Service*. https://www.cas.org/cas-solutions-login (accessed 2024-03-24).
(39) McLean, R. J.; Pierson, L. S., III; Fuqua, C. A simple screening protocol for the identification of quorum signal antagonists. *J. Microbiol. Methods* **2004**, *58* (3), 351.
(40) *Protein Data Bank Homepage*. https://www.rcsb.org/ (accessed 2023-11-10).
(41) Gohlke, H.; Hendlich, M.; Klebe, G. Knowledge-based scoring function to predict protein-ligand interactions. *J. Mol. Biol.* **2000**, *295* (2), 337.
(42) Casillas-Vargas, G.; Ocasio-Malavé, C.; Medina, S.; Morales-Guzmán, C.; Del Valle, R. G.; Carballeira, N. M.; Sanabria-Ríos, D. J. Antibacterial fatty acids: An update of possible mechanisms of action and implications in the development of the next-generation of antibacterial agents. *Prog. Lipid Res.* **2021**, *82*, 101093.
(43) Devescovi, G.; Kojic, M.; Covaceuszach, S.; Camara, M.; Williams, P.; Bertani, I.; Subramoni, S.; Venturi, V. Negative regulation of volacein biosynthesis in *Chromobacterium violaceum*. *Front. Microbiol.* **2017**, *8*, 349.
(44) Stauff, D. L.; Bassler, B. L. Quorum sensing in *Chromobacterium violaceum*: DNA recognition and gene regulation by the CviR receptor. *J. Bacteriol.* **2011**, *193* (15), 3871.
(45) Papenfort, K.; Bassler, B. L. Quorum sensing signal-response systems in Gram-negative bacteria. *Nat. Rev. Microbiol.* **2016**, *14* (9), 576.

https://doi.org/10.1021/acsomega.4c01121
ACS Omega 2024, 9, 32536−32546